


## Stability of the particle-hole Pfaffian state and the $\frac{5}{2}$ -fractional quantum Hall effect

Edward H. Rezayi<sup>1</sup>, Kiryl Pakrouski<sup>2</sup>, and F. D. M. Haldane<sup>2</sup><sup>1</sup>*Department of Physics, California State University Los Angeles, Los Angeles, California 90032, USA*<sup>2</sup>*Department of Physics, Princeton University, Princeton, New Jersey 08544, USA*
 (Received 24 June 2021; revised 5 August 2021; accepted 6 August 2021; published 23 August 2021)

We present a method for the exact construction of the fully particle-hole symmetric Pfaffian (PH-Pfaffian) ground state and its charged excitations on a sphere. We adopt the Moore-Read state, but with a nonholomorphic pairing component as in previous studies, and project it to the lowest Landau level. We study the energetics as well as other properties of these states and find that in a pure system interacting with the Coulomb forces the PH-Pfaffian cannot compete with either the Moore-Read state or its particle-hole conjugate, the anti-Pfaffian state, as an explanation for the  $\frac{5}{2}$  effect.

DOI: [10.1103/PhysRevB.104.L081407](https://doi.org/10.1103/PhysRevB.104.L081407)

One of the most intriguing topological [1] quantum phases of matter was discovered [2] in the fractional quantum Hall effect (FQHE) [3,4] at  $\frac{5}{2}$  filling of the lowest two Landau levels (LLs). A large number of studies of the  $\frac{5}{2}$  state point to either the Moore-Read [5] Pfaffian (MR-Pf) state, or its particle-hole (PH) conjugate, the anti-Pfaffian (aPf) state [6,7] to explain this phenomenon. Another related state that has recently attracted considerable attention is the PH-Pfaffian [8] (PH-Pf). It is so named because, unlike the MR or the aPf, this state is symmetric under PH conjugation. All three are expected to be Hall superconductors [9], but with different pairing symmetries. There is however scant support in numerical studies of the  $\frac{5}{2}$  state for the PH-Pfaffian. Instead, there is considerable evidence in favor of the MR and aPf. Some examples in different geometries are given in Refs. [10–15].

Earlier studies, for the most part, preserved the PH symmetry of the Hamiltonian and were unable to discriminate between the latter two ground states. In the presence of inter-Landau-level transitions or mixing (a ubiquitous feature of experiments), PH symmetry is broken and the aPf gains the advantage [16–18]. However, the energy splitting per particle is small and omitting some pseudopotential components of the three-body mixing [19] corrections stabilizes [20] the MR-Pf [21–23]. The quasiparticle excitations of all three states possess Majorana zero modes and are expected to obey non-Abelian statistics [5,24], which is a necessary ingredient for quantum information processing. They are also fully spin polarized, in agreement with both experiment [25,26] and numerical calculations [10,27] of the  $\frac{5}{2}$  effect.

Recent measurements [28] of quantized thermal Hall conductance  $\kappa_{xy}$ , however, found a value that is only consistent with the PH-Pf state. There are several interesting scenarios for explaining this observation. Disorder, which is present in experiment, was first put forward as the decisive factor in stabilizing the PH-Pf [29]. Alternate scenarios that favor the PH-Pf ground state have also been suggested [30,31]. A different possibility is the formation of Pf and aPf domains

in the presence of disorder [32–34], which under suitable conditions could result in the measured quantized thermal Hall conductance. Whether this mechanism can account for the experimental observation is unclear [35,36].

Another possibility is that the aPf ground state, under certain conditions, could produce the measured  $\kappa_{xy}$  [37,38]. However, a more recent experiment also supports a PH-Pf ground state [39]. In any event, these developments call for a thorough examination of the PH-Pfaffian state.

In this Letter we formulate an exact procedure for calculating the ground state and charged quasiparticle excited states of the PH-Pfaffian. We then obtain results for up to 14- and 12-electron systems for the ground and charged excited states, respectively. These sizes are comparable to previous exact diagonalization studies of the  $\frac{5}{2}$  effect. We use the spherical geometry since the angular momentum “technology” simplifies the construction. In what follows, all energies are given in units of  $e^2/4\pi\epsilon\ell_B$ . Distances (wave vectors) are given in units of the magnetic length  $\ell_B$  (inverse magnetic length) and densities in inverse  $2\pi\ell_B^2$  units. As a reminder, Fig. 1 shows the gapped phases of FQHE near the half-filled first excited Landau level (1LL) as the first Haldane pseudopotential  $v_1$  is varied. Only the first three odd pseudopotentials seem substantially different from their lowest-Landau-level (LLL) values. The arrows show the positions of the MR, PH-Pfaffian, and the anti-Pfaffian from left to right, respectively. The only visibly gapped states appear to be MR-Pf and aPf, which are related by particle-hole conjugation that maps the electrons to holes and vice versa. The MR-Pf satisfies the relation  $N_\phi = 2N_e - 3$ , which has a shift of 3. The shifts of the PH-Pf and aPf are 1 and  $-1$ , respectively. Different shifts generally signify a different topological phase of matter.

*Computation of wave function.* While there may well be other forms for the PH-Pf wave function we will use the one from previous studies [29,40–42],

$$|\Psi_{\text{PH-Pf}}(\{\mathbf{r}_i\})\rangle = \text{Pf}_{i,j} \left\{ \frac{1}{\bar{u}_i \bar{v}_j - \bar{u}_j \bar{v}_i} \right\} |\Psi_{1/2}\rangle, \quad (1)$$

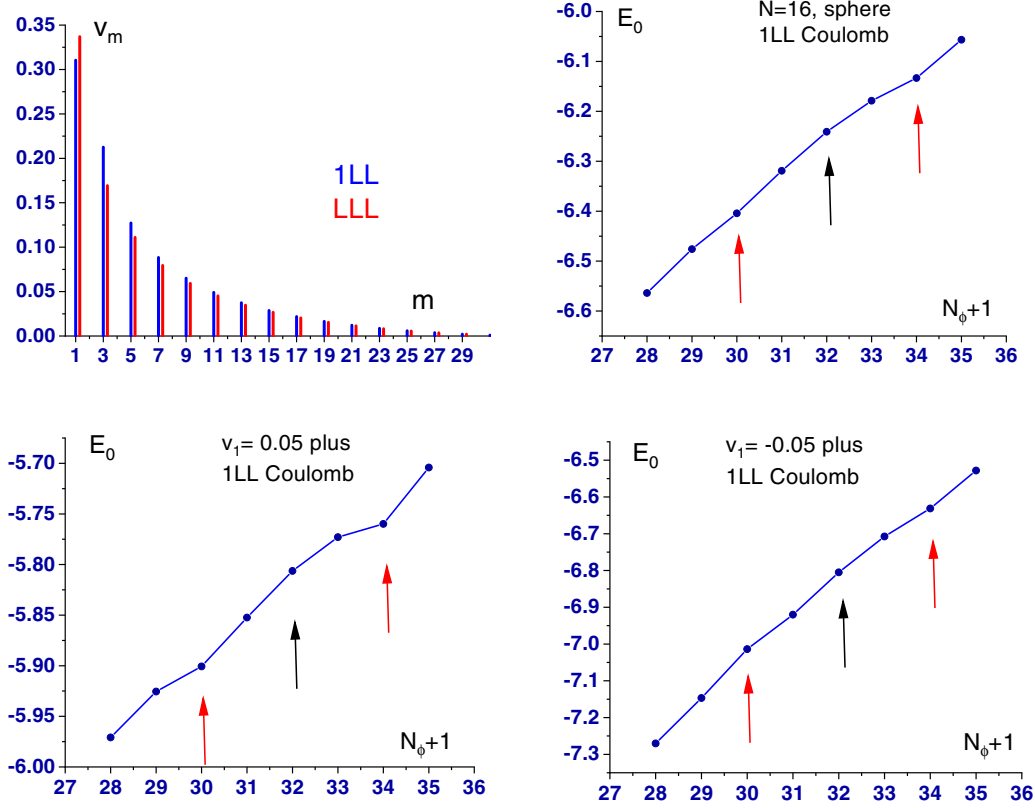


FIG. 1. Top left: In the first row, a comparison of pseudopotentials  $v_m$ , for spin-polarized electrons of the lowest and first excited Landau levels. Top right: Ground state energies for the Coulomb potential in 1LL as the flux  $N_\phi$  is varied for 16 electrons. Bottom:  $v_1$  of 1LL Coulomb is varied by  $\pm 0.05$ .

where  $u$  and  $v$  are spinor coordinates [43] and the holomorphic part  $|\Psi_{1/2}\rangle$  is the  $\nu = 1/2$  bosonic Laughlin state:

$$|\Psi_{1/2}(\{u_i, v_i\})\rangle = \prod_{i>j} (u_i v_j - u_j v_i)^2. \quad (2)$$

Projection of the wave function to the LLL turns  $\bar{u}$  and  $\bar{v}$  into operators (usually derivatives [44]). The key idea in our approach is to project one pair at a time in occupation space. The projection operators are only in the Pfaffian, which is the pairing part of the wave function. We thus start with projecting a single pair. Multiplying both the numerator and denominator by the factor  $u_i v_j - u_j v_i$ , we have

$$\frac{1}{\bar{u}_i \bar{v}_j - \bar{u}_j \bar{v}_i} = \frac{u_i v_j - u_j v_i}{|u_i v_j - u_j v_i|^2}. \quad (3)$$

TABLE I. Some attributes, indicated by the column headings, of PH-Pf and MR states for different sizes  $N_e$ .

$N_e$	$ \langle \Psi   \Psi_{\text{Sym}} \rangle $	Variational $E_0$	$E_0/N_e$	$E_0(\text{Pf})/N_e$
6	0.9999996	-2.583729	-0.4306215	-0.4868794
8	0.9999633	-3.291081	-0.4113851	-0.4458210
10	0.9999807	-3.993417	-0.3993417	-0.4248679
12	0.9999463	-4.694213	-0.3911844	-0.4122298
14	0.9998940	-5.404673	-0.3860481	-0.4040570

This is a rotationally invariant holomorphic pair (scalar) operator with a  $1/r^2$  potential, where  $r$  is the chord distance between particles  $i$  and  $j$  on a unit sphere. This potential is to be projected into the LLL. The numerator is holomorphic and turns a two-boson state into a state of two fermions, which in total adds a flux quantum  $N_\phi^F = N_\phi^B + 1$ , without altering  $J$  and  $M$ :  $|J, M, N_\phi^B\rangle$  transforms to  $|J, M, N_\phi^F\rangle$ .  $J$  and  $M$  are the total and azimuthal angular momenta of the pair. Using

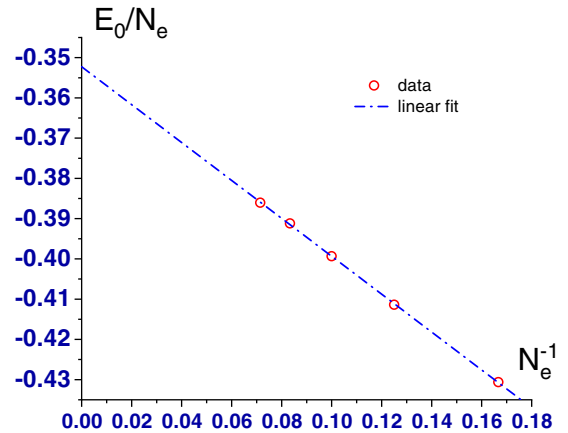


FIG. 2. Variational energies of the PH-Pfaffian state for 6–14 electrons. The straight line is a least-squares fit of the data, yielding an infinite-size value of  $-0.3523 \pm 0.0004$  per electron.

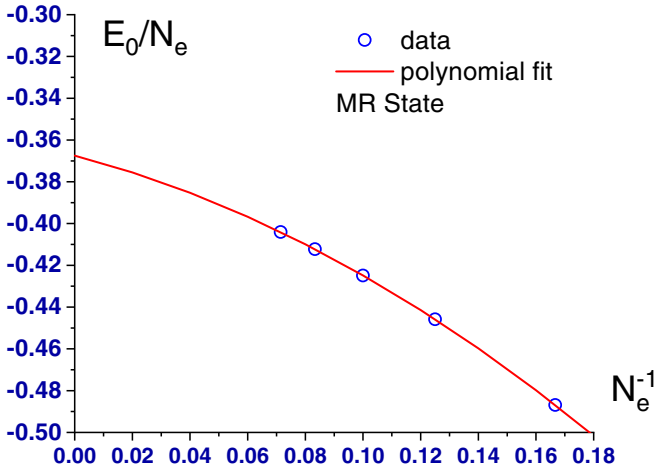


FIG. 3. Variational energies of the MR-Pfaffian state for 6–14 electrons. The curve is a fit of the data to a polynomial of degree 2. The intercept in the infinite-size limit is  $-0.3675 \pm 0.0004$  per electron.

the Wigner-Eckart theorem we obtain the reduced matrix elements below. These are, in fact, the Haldane pseudopotentials for a  $1/r^2$  “Hamiltonian” that changes a pair of bosons into a pair of fermions. Therefore, we set  $M = J$ , simplifying the two-particle wave functions [43] to

$$|J, J; N_\phi^{B(F)}\rangle = (u_i v_j - u_j v_i)^{N_\phi^{B(F)} - J} u_i^J u_j^J, \quad (4)$$

where  $B(F)$  refers to bosons (fermions). The number of bosons and fermions is equal and is denoted by  $N_e$ . The matrix element of the pair operator between the two-particle states is reduced to the expectation value of  $1/r^2$  (apart from normalization factors) for a two-fermion state. The pseudopotentials are

$$V_J = \frac{N_\phi^F + 1}{\sqrt{(N_\phi^F - J)(N_\phi^F + 1 + J)}}. \quad (5)$$

To get the matrix elements in a more convenient form [Eq. (6)], we expand the pair creation annihilation operators in terms of a pair of single-particle boson annihilation and

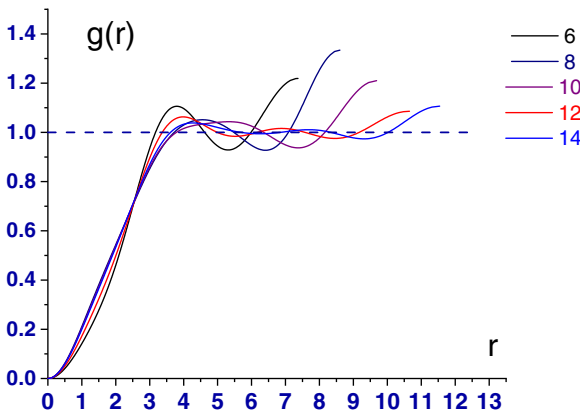


FIG. 4. Pair correlation function for 6–14 electrons as a function of the large circle distance.

a pair of fermion creation operators. Again, because of the additional flux quantum for fermions relative to bosons, the needed Clebsch-Gordan (CG) coefficients for the same  $J$  and  $M$  have the correct parity under particle exchange for both bosons and fermions. Combining the CG coefficients with  $V_J$  and summing over  $J$  and  $M$  yields the desired matrix elements, which can be separately calculated and stored:

$$V(m_i^f, m_j^f; m_i^b, m_j^b) = \left\langle m_i^f, m_j^f \left| \frac{u_i v_j - u_j v_i}{|u_i v_j - u_j v_i|^2} \right| m_i^b, m_j^b \right\rangle, \\ m_i^f + m_j^f = m_i^b + m_j^b. \quad (6)$$

The matrix elements can easily be antisymmetrized in the two-fermion and symmetrized in the two-boson orbitals.

The coordinates in the Pfaffian can now be integrated out. The antisymmetrization required in the Pfaffian can, by a change of integration variables, be compensated by the exchange of fermion orbitals. The interpair antisymmetrization of the fermion orbitals only requires  $N_{\text{fact}} = N_e! / [2^{N_e/2} (N_e/2)!] = (N_e - 1)!!$  independent terms, which is much smaller than  $N_e!$ . However, this operation has to be done for all occupied single-particle states with total zero azimuthal angular momentum. The total number of configurations for fermions is  $Nc = N_{\text{fact}} N_H$ , where  $N_H$  is the dimension of the appropriate many-body fermion Hilbert space [45].

The main calculation is organized in a *single* loop of size  $Nc$  for fermions. Because of the conservation law for each pair of bosons in Eq. (6), there are an additional  $N_e/2$  inner loops for boson orbitals. In the inner core of these  $N_e/2 + 1$  loops the PH-Pf wave function is obtained from the product of the matrix elements, other information on the fermion basis, and the Laughlin wave function.

While the code is very short and relatively simple, it still is an  $N_e$ -body operator with a much higher degree of complexity than diagonalizing a many-body Hamiltonian. On the other hand, the computations for different sets of fermion orbitals  $\{m_i^f\}$  are *independent* and the outer loop can be massively parallelized. We have also taken advantage of reflection symmetry to divide the basis (by its parity), and hence the outer fermion loop, into two independent but nearly equal parts, providing further parallelization.

*The ground state (GS).* The PH-Pfaffian wave functions are very nearly particle-hole symmetric. However, they cannot be fully symmetrized or antisymmetrized by the usual means (making a linear combination of the two states) because of the antiunitarity of the PH transformation. The problem is overcome if the eigenvectors of the  $2 \times 2$  overlap matrix of the two states related by PH conjugation are obtained. The parity of the state is immaterial. One eigenvector would have an overlap of near unity with the calculated wave function (see Table I) and the other a very small overlap. The table also shows their variational energies for the 1LL Coulomb potential. These are plotted in Fig. 2 and give an extrapolation to an infinite size of  $-0.3523$ . That is larger than  $-0.3675$  for the Pf (or equivalently for aPf) energies extrapolated in Fig. 3. We note that the PH-Pf on the sphere is aliased (same  $N_e$  and  $N_\phi$ ) with the particle-hole symmetric version of Jain’s [46] composite fermion (CF) with an effective magnetic flux quantum of one:  $N_\phi^* = N_\phi - 2(N_e - 1) = 1$  as opposed to zero [47,48]. This has been called the Dirac CF (DCF) [8,49]

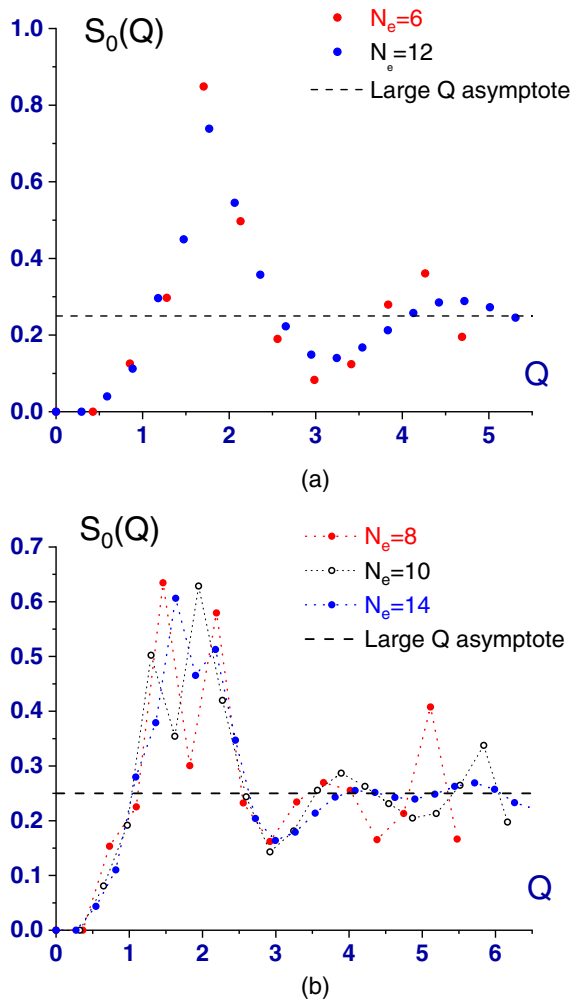


FIG. 5. (a) Guiding center structure factor with a single main peak for  $N_e = 6$  and 12. (b) Same as in (a) except with two main peaks for  $N_e = 8, 10$ , and 14. Solid (open) symbols are for cases where the larger peak is to the left (right) of the other main peak. The dotted line is the known asymptotic value [53] of  $S_0(Q)$  for large wave vectors  $Q$ .

since its Berry phase, when taken around the Fermi surface, is  $\pi$  [8,50,51]. Both composite Fermi liquids of CF and DCF are appropriate ground states in the LLL at  $\nu = \frac{1}{2}$  but not at  $\frac{5}{2}$  filling. In the PH-symmetric case the electrons form closed shells with total angular momentum  $L = 0$  for sizes given by  $N_e = (n+1)(n+2)$ , with  $n$  a non-negative integer. For partially filled shells, the inter-DCF distances can be maximized for nonzero values of angular momentum, which vary systematically with size [48].

Figure 4 shows the pair correlation function for even sizes of 6–14 electrons. Oddly, there is no indication of convergence, in sharp contrast to the case of the MR-Pf state, where a clear picture emerges with 12 electrons [52]. In addition, long-range tail oscillations, which are typical of composite Fermi liquids [48], persist to large sizes [42]. Also, there appears to be two classes of states determined by whether or not the DCFs form a closed shell. Figure 5 shows the (LL-independent) guiding center structure factor  $S_0(Q)$ . We separate the filled shell configurations  $N_e = 6$  and 12 ( $n = 1$

TABLE II. The variational energies of GS, charge excitations, and the gaps of PH-Pf and MR state for 12 electrons.

State	QE energy	QH energy	GS energy	$\Delta_c$
PH-Pf	-4.774736	-4.615954	-4.694213	-0.001132
MR-Pf	-5.028995	-4.833692	-4.946758	0.015415

and 2, respectively) from the rest. Only the first group exhibits a single sharp peak at a wave vector that approaches  $2k_f$  for large sizes. This separation agrees with the high overlap of DCF with the PH-Pf for  $N_e = 12$  obtained by the Monte Carlo method [40]. Since the PH-Pf is in fact a paired state of DCFs, this trend is not entirely surprising. For unfilled shells the angular momentum of DCF is nonzero and thus will have no overlap with the PH-Pf GS. However, these trends may not bode well for a gapped topological phase. Moreover, the  $n = 1$  LL Coulomb potential is insufficient for the pairing of DCFs into a Hall superconductor and it is left as a compressible state. It seems unlikely that disorder can overcome these shortcomings.

*Charge excitations.* To complete the picture of the PH-Pf, we turn to the quasielectron and quasihole excitations. These, given below, are the most natural extension of the ground state wave function,

$$|\Psi_{\text{QE}}(\mathbf{r}_i)\rangle = \text{Pf}_{i,j} \left\{ \frac{\bar{u}_i \bar{v}_j + \bar{u}_j \bar{v}_i}{\bar{u}_i \bar{v}_j - \bar{u}_j \bar{v}_i} \right\} |\Psi_{1/2}\rangle, \quad (7)$$

and

$$|\Psi_{\text{QH}}(\mathbf{r}_i)\rangle = \text{Pf}_{i,j} \left\{ \frac{u_i v_j + u_j v_i}{\bar{u}_i \bar{v}_j - \bar{u}_j \bar{v}_i} \right\} |\Psi_{1/2}\rangle. \quad (8)$$

The two quasiparticles are at the poles of the sphere. As a result, the full rotational symmetry is downgraded to azimuthal symmetry. We have included the corresponding MR quasiparticle states for comparison. The wave function of a pair of quasielectrons and quasiholes [14,52] is the same as in Eqs. (7) and (8), but with holomorphic denominators [54]. The calculation becomes a little more complicated, due to the loss of full rotational symmetry, but the matrix elements of the two-body interactions can still be computed by the transformation of coordinates [55]. Figure 6 shows the densities of these states for  $N_e = 12$ . We also compare the variational energies in Table II. Again, the MR state and the corresponding quasiparticles have lower energies. Whether they remain so in the thermodynamic limit is unclear. A more meaningful comparison would be to calculate the energy gap for creating a neutral pair of quasielectrons and quasiholes. Since a pair of quasiparticles is created for each quantum of flux above or below the GS, we divide the energies by two. The energy gap for creating the neutral pair is defined by

$$\Delta_c = \frac{E(N_\phi + 1, N_e) + E(N_\phi - 1, N_e) - 2E(N_\phi, N_e)}{2}, \quad (9)$$

where  $N_\phi$  is the number of flux quanta for the ground state. We have used the actual values of the energies without any subtractions or rescaling. The last column of Table II shows the results for both PH-Pf and MR for 12 electrons. A more telling picture of the gaps as a function of inverse size is

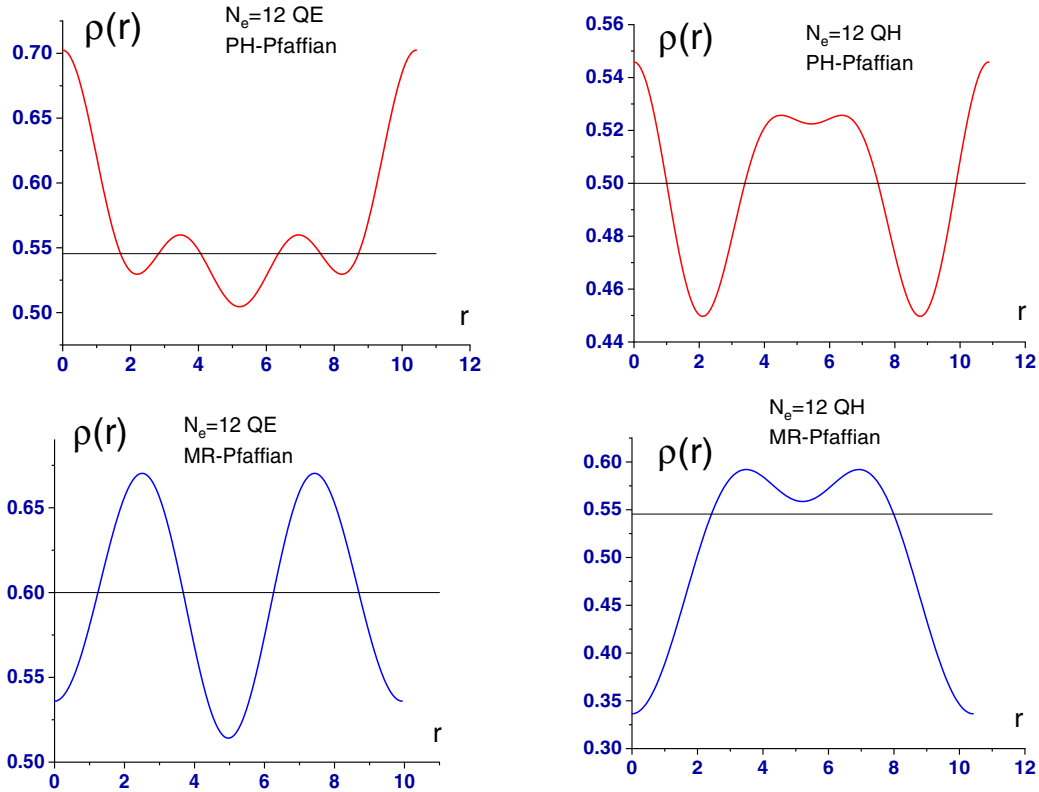


FIG. 6. The density of the PH-Pf (upper figures) two quasielectrons (QEs) and two quasiholes (QHs) for 12 electrons as a function of the large circle distances. The horizontal lines mark the density of the fluid if the charge was distributed uniformly. The lower two figures are the MR QEs and QHs densities.

shown in Fig. 7 for 8-, 10-, and 12-electron systems. The stark difference in the energy gaps between the MR-Pf (or aPf) and the PH-Pf is clearly visible.

Finally, we note that recent measurements [56] on a closely related system appear to be consistent with our results. The experiment by Huang and co-workers on half-filled 1LL in bilayer graphene did not find any evidence for the PH-Pf. Instead, depending on the valley Zeeman splitting, they found

either the MR-Pf (at  $\nu = \frac{3}{2}$  and  $\frac{7}{2}$ ) or the aPf (at  $\nu = \frac{5}{2}$ ), which were identified by the presence of their respective daughter states.

In summary, we have presented an exact method for projecting the PH-Pfaffian as well as its quasiparticle states to the lowest Landau level. The calculations can be organized in a way that is scalable on massively parallel machines [57]. We obtained wave functions for up to 14 and 12 electrons for the GS and charge excitations, respectively. By extrapolating finite-size results to large sizes in a pure system, we unequivocally find that the PH-Pf energetically falls short of the Moore-Read Pf (or aPf) state. Other factors such as Landau-level mixing or disorder are unlikely to reverse these trends. Including LL-mixing corrections [19] with three-body interactions for up to a relative angular momentum  $M = 9$  (as in Ref. [18]) shows no indication of stabilizing the PH-Pf. A more comprehensive study of LL mixing will be reported elsewhere [58].

We thank S. Simon, M. Zaletel, Z. Papić, and J. Wang for helpful discussions. The authors gratefully acknowledge DOE support under Grant No. DE-SC0002140. K.P. was also supported by the Swiss National Science Foundation through the Early Postdoc.Mobility Grant No. P2EZP2\_172168. The simulations presented in this Letter were performed on computational resources managed and supported by Princeton's Institute for Computational Science & Engineering and OIT Research Computing.

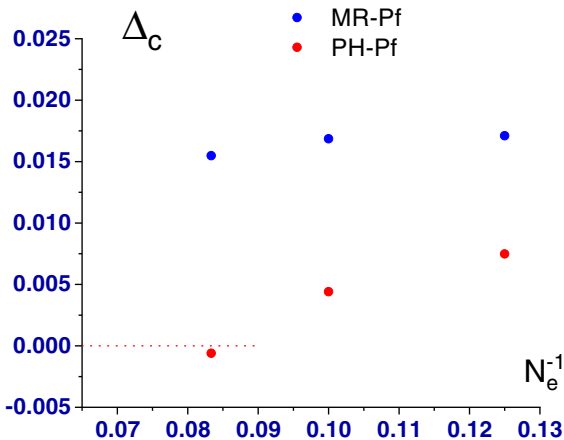


FIG. 7. Charge gaps in 8–12 electron systems for both MR and PH-Pf states.

- [1] X. G. Wen, *Int. J. Mod. Phys. B* **04**, 239 (1990); **06**, 1711 (1992).
- [2] R. Willett, J. P. Eisenstein, H. L. Störmer, D. C. Tsui, A. C. Gossard, and J. H. English, *Phys. Rev. Lett.* **59**, 1776 (1987).
- [3] C. Nayak, S. H. Simon, A. Stern, M. Freedman, and S. Das Sarma, *Rev. Mod. Phys.* **80**, 1083 (2008).
- [4] T. H. Hansson, M. Hermanns, S. H. Simon, and S. F. Viefers, *Rev. Mod. Phys.* **89**, 025005 (2017).
- [5] G. Moore and N. Read, *Nucl. Phys. B* **360**, 362 (1991).
- [6] M. Levin, B. I. Halperin, and B. Rosenow, *Phys. Rev. Lett.* **99**, 236806 (2007).
- [7] S.-S. Lee, S. Ryu, C. Nayak, and M. P. A. Fisher, *Phys. Rev. Lett.* **99**, 236807 (2007).
- [8] D. T. Son, *Phys. Rev. X* **5**, 031027 (2015).
- [9] N. Read and D. Green, *Phys. Rev. B* **61**, 10267 (2000).
- [10] R. H. Morf, *Phys. Rev. Lett.* **80**, 1505 (1998).
- [11] E. H. Rezayi and F. D. M. Haldane, *Phys. Rev. Lett.* **84**, 4685 (2000).
- [12] A. E. Feiguin, E. Rezayi, C. Nayak, and S. Das Sarma, *Phys. Rev. Lett.* **100**, 166803 (2008).
- [13] M. R. Peterson, T. Jolicoeur, and S. Das Sarma, *Phys. Rev. Lett.* **101**, 016807 (2008).
- [14] X. Wan, Z.-X. Hu, E. H. Rezayi, and K. Yang, *Phys. Rev. B* **77**, 165316 (2008).
- [15] J. Zhao, D. N. Sheng, and F. D. M. Haldane, *Phys. Rev. B* **83**, 195135 (2011).
- [16] S. H. Simon and E. H. Rezayi, *Phys. Rev. B* **87**, 155426 (2013); E. H. Rezayi and S. H. Simon, *Phys. Rev. Lett.* **106**, 116801 (2011).
- [17] M. P. Zaletel, R. S. K. Mong, F. Pollmann, and E. H. Rezayi, *Phys. Rev. B* **91**, 045115 (2015).
- [18] E. H. Rezayi, *Phys. Rev. Lett.* **119**, 026801 (2017).
- [19] I. Sodemann and A. H. MacDonald, *Phys. Rev. B* **87**, 245425 (2013).
- [20] If the first five as opposed to six or more three-body pseudopotentials are included [58].
- [21] K. Pakrouski, M. R. Peterson, T. Jolicoeur, V. W. Scarola, C. Nayak, and M. Troyer, *Phys. Rev. X* **5**, 021004 (2015).
- [22] M. R. Peterson and C. Nayak, *Phys. Rev. B* **87**, 245129 (2013).
- [23] A. Wójs, C. Tóke, and J. K. Jain, *Phys. Rev. Lett.* **105**, 096802 (2010).
- [24] P. Bonderson, V. Gurarie, and C. Nayak, *Phys. Rev. B* **83**, 075303 (2011).
- [25] L. Tiemann, G. Gamez, N. Kumada, and K. Muraki, *Science* **335**, 828 (2012).
- [26] J. P. Eisenstein, L. N. Pfeiffer, and K. W. West, *Phys. Rev. Lett.* **118**, 186801 (2017).
- [27] A. E. Feiguin, E. Rezayi, K. Yang, C. Nayak, and S. Das Sarma, *Phys. Rev. B* **79**, 115322 (2009).
- [28] M. Banerjee, M. Heiblum, V. Umansky, D. E. Feldman, Y. Oreg, and A. Stern, *Nature (London)* **559**, 205 (2018).
- [29] P. T. Zucker and D. E. Feldman, *Phys. Rev. Lett.* **117**, 096802 (2016).
- [30] L. Antonić, J. Vučićević, and M. V. Milovanović, *Phys. Rev. B* **98**, 115107 (2018).
- [31] P.-S. Hsin, Y.-H. Lin, N. M. Paquette, and J. Wang, *Phys. Rev. Research* **2**, 043242 (2020).
- [32] C. Wang, A. Vishwanath, and B. I. Halperin, *Phys. Rev. B* **98**, 045112 (2018).
- [33] D. F. Mross, Y. Oreg, A. Stern, G. Margalit, and M. Heiblum, *Phys. Rev. Lett.* **121**, 026801 (2018).
- [34] B. Lian and J. Wang, *Phys. Rev. B* **97**, 165124 (2018).
- [35] S. H. Simon, M. Ippoliti, M. P. Zaletel, and E. H. Rezayi, *Phys. Rev. B* **101**, 041302(R) (2020).
- [36] W. Zhu, D. N. Sheng, and K. Yang, *Phys. Rev. Lett.* **125**, 146802 (2020).
- [37] S. H. Simon and B. Rosenow, *Phys. Rev. Lett.* **124**, 126801 (2020).
- [38] H. Asasi and M. Mulligan, *Phys. Rev. B* **102**, 205104 (2020).
- [39] B. Dutta, W. Yang, R. A. Melcer, H. K. Kundu, M. Heiblum, V. Umansky, Y. Oreg, A. Stern, and D. Mross, [arXiv:2101.01419](https://arxiv.org/abs/2101.01419).
- [40] R. V. Mishmash, D. F. Mross, J. Alicea, and O. I. Motrunich, *Phys. Rev. B* **98**, 081107(R) (2018).
- [41] A. C. Balram, M. Barkeshli, and M. S. Rudner, *Phys. Rev. B* **98**, 035127 (2018).
- [42] M. Yutushui and D. F. Mross, *Phys. Rev. B* **102**, 195153 (2020).
- [43] F. D. M. Haldane, *Phys. Rev. Lett.* **51**, 605 (1983).
- [44] J. K. Jain and R. K. Kamilla, *Phys. Rev. B* **55**, R4895(R) (1997).
- [45] The relevant information on fermions can be calculated separately and stored (in a piecemeal manner if necessary). Several of the fermion occupations, permutation signs, and hashtag addresses can be stored within integers.
- [46] J. K. Jain, *Phys. Rev. Lett.* **63**, 199 (1989).
- [47] B. I. Halperin, P. A. Lee, and N. Read, *Phys. Rev. B* **47**, 7312 (1993).
- [48] E. Rezayi and N. Read, *Phys. Rev. Lett.* **72**, 900 (1994).
- [49] S. D. Geraedts, M. P. Zaletel, R. S. K. Mong, M. A. Metlitski, A. Vishwanath, and O. I. Motrunich, *Science* **352**, 197 (2016).
- [50] S. D. Geraedts, J. Wang, E. H. Rezayi, and F. D. M. Haldane, *Phys. Rev. Lett.* **121**, 147202 (2018).
- [51] J. Wang, S. D. Geraedts, E. H. Rezayi, and F. D. M. Haldane, *Phys. Rev. B* **99**, 125123 (2019).
- [52] N. Read and E. Rezayi, *Phys. Rev. B* **54**, 16864 (1996).
- [53] In this version the normalization of  $S_0$  has been changed from  $N_e$  to  $N_\phi$ . See F. D. M. Haldane, The hierarchy of fractional states and numerical studies, in *The Quantum Hall Effect*, edited by R. E. Prange and S. M. Girvin, Graduate Texts in Contemporary Physics (Springer, New York, 1990), p. 303.
- [54] The spherical version of the wave function on the disk can be obtained by stereographic projection. The two poles are mapped to infinity (north pole) and to the origin. In the notation of Ref. [52] the (complex) positions of the quasiholes  $w_1 \rightarrow 0$  and  $w_2$  becomes an overall factor, which can be dropped. This yields the form in Ref. [14] used in this Letter.
- [55] G. Fano, F. Ortolani, and E. Colombo, *Phys. Rev. B* **34**, 2670 (1986).
- [56] K. Huang, H. Fu, D. R. Hickey, N. Alem, X. Lin, K. Watanabe, T. Taniguchi, and J. Zhu, [arXiv:2105.07058](https://arxiv.org/abs/2105.07058).
- [57] A similar approach can be used to perform the exact projection of Jain states to the LLL for comparable sizes done here.
- [58] K. Pakrouski, A. Valdez, M. R. Peterson, and E. H. Rezayi (unpublished). This work includes the first 11 three-body pseudopotentials.